

miRNA signature identification of retinoblastoma and the correlations between differentially expressed miRNAs during retinoblastoma progression

Yang Yang,¹ Qi Mei²

¹Department of Ophthalmology, Renmin Hospital of Wuhan University, Wuhan, China; ²Department of Oncology, Tongji Hospital, Tongji Medical College, Huazhong University of Science and Technology, Wuhan, China

Purpose: Retinoblastoma (RB) is a common pediatric cancer. The study aimed to uncover the mechanisms of RB progression and identify novel therapeutic biomarkers.

Methods: The miRNA expression profile GSE7072, which includes three RB samples and three healthy retina samples, was used. After data normalization using the preprocessCore package, differentially expressed miRNAs (DE-miRs) were selected by the limma package. The targets of the DE-miRs were predicted based on two databases, followed by construction of the miRNA–target network. Pathway enrichment analysis was conducted for the targets of the DE-miRNAs using DAVID. The CTD database was used to predict RB-related genes, followed by clustering analysis using the pvclust package. The correlation network of DE-miRs was established. MiRNA expression was validated in another data set, GSE41321.

Results: In total, 24 DE-miRs were identified whose targets were correlated with the cell cycle pathway. Among them, *hsa-miR-373*, *hsa-miR-125b*, and *hsa-miR-181a* were highlighted in the miRNA–target regulatory network; 14 DE-miRs, including *hsa-miR-373*, *hsa-miR-125b*, *hsa-miR-18a*, *hsa-miR-25*, *hsa-miR-20a*, and *hsa-let-7 (a, b, c)*, were shown to distinguish RB from healthy tissue. In addition, *hsa-miR-25*, *hsa-miR-18a*, and *hsa-miR-20a* shared the common target *BCL2L1*; *hsa-let-7b* and *hsa-miR-125b* targeted the genes *CDC25A*, *CDK6*, and *LIN28A*. Expression of three miRNAs in GSE41321 was consistent with that in GSE7072.

Conclusions: Several critical miRNAs were identified in RB progression. *Hsa-miR-373* might regulate RB invasion and metastasis, *hsa-miR-181a* might involve in the *CDKN1B*-mediated cell cycle pathway, and *hsa-miR-125b* and *hsa-let-7b* might serve as tumor suppressors by coregulating *CDK6*, *CDC25A*, and *LIN28A*. The miRNAs *hsa-miR-25*, *hsa-miR-18a*, and *hsa-miR-20a* might exert their function by coregulating *BCL2L1*.

Retinoblastoma (RB) is the most common pediatric malignancy. The epidemiology of RB has been investigated in many population-based studies, and the incidence rate of RB is estimated at 40–60 cases per million live births in the world [1-4]. Although the mortality rate is low in patients with RB who receive aggressive multimodal therapy, in developed countries, nearly half of patients with advanced bilateral RB suffer from partial or full sight loss [5]. In developing countries, because the disease is often diagnosed at later stages, the survival rate is lower than in developed countries [6].

To reduce morbidity and preserve the sight of a child during the early stages of RB, numerous studies have explored more effective approaches, such as targeted therapy using bioinformatics methods. For instance, combining epigenetic analysis with gene expression analysis, Zhang et al. identified

the important oncogene *spleen tyrosine kinase (SYK)* (Gene ID: 6850; OMIM: 600085), which is elevated in RB and essential for RB tumor cell survival [7]. Another study also discovered 119 candidate genes, such as *CDC25C* (Gene ID: 995, OMIM: 157680), *CDC6* (Gene ID: 990, OMIM: 602627), and *TP53* (Gene ID: 7157 OMIM: 191170), for RB diagnosis [8]. MicroRNAs (miRNAs) are small noncoding RNAs that play significant roles in cellular functions and physiology. By regulating the expression of the target genes, miRNAs are confirmed to be involved in the development of various cancers, and thus have been suggested as tumor biomarkers [9,10]. Several miRNAs such as *miR-30*, *miR-let-7e*, *miR-21*, and *miR-320* are dysregulated in RB samples and have been supposed to be diagnostic biomarkers for detecting RB [11,12]. Downregulated *miR-204* is another indicator in RB prediction [13]. Martin et al., using a TaqMan Low Density Array, discovered a total of 41 differentially expressed miRNAs (DE-miRs) between 12 RB samples and three healthy retina samples in humans, including 13 previously identified miRNAs (*miR-17*, *miR-20b*, *miR-22*, *miR-25*, *miR-34a*, *miR-34c-5p*, *miR-106a*, *miR-106b*, *miR-93*, *miR-129*,

Correspondence to: Qi Mei, Department of Oncology, Tongji Hospital, Tongji Medical College, Huazhong University of Science and Technology, Jiefang Avenue 1095, Wuhan 430030, China; Phone: +86-027-83663407; FAX: +86-027-83662834; email: borismq@163.com

miR-193-5p, *miR-342-5p*, *miR-370*) in human and mouse RB and many novel miRNAs, such as *miR-18a*, *miR-138*, *miR-155*, *miR-382*, and *miR-504* [14]. Additionally, the *miR-17-92* cluster has been demonstrated as an RB-collaborating gene that promotes RB development [15]. More recently, another 18 miRNAs have been newly implicated in RB and have great potential to serve as signatures in the detection of this disease [16]. However, the target genes of these miRNAs are rarely reported. Notably, using paired mRNA and miRNA expression profiles, Huang et al. identified several targets of miRNAs in RB samples and further verified *CDC25A* (Gene ID: 993 OMIM: 116947) and *BCL7A* (Gene ID: 605 OMIM: 601406) are the target genes of *let-7b* [17]. However, the researchers emphasized the roles of miRNA *let-7b* and did not mention other potential miRNAs or the correlations between them. In addition, the detailed regulation mechanisms of miRNAs to RB remain obscure.

Therefore, we reanalyzed the miRNA expression profile GSE7072 [17] to obtain more relevant miRNAs using differential analysis. The targets of these miRNAs were also predicted using two experimental validated databases (miRecords and MirWalk). Relationships between these miRNAs were further explored to comprehensively uncover the underlying mechanisms of RB progression. We aimed to find novel miRNA biomarkers for the prevention and prognosis of RB development.

METHODS

A flowchart of the analyses in the study is shown in Figure 1.

Microarray data: The miRNA expression profile data with the accession number GSE7072 [17], which is available in the public Gene Expression Omnibus (GEO) database, was employed in the present study. The data set comprised the total RNA information of a cohort of 160 human miRNAs from three RB samples and three replicates of a healthy retina, based on the platform of the GPL4879Human miRNA

2k custom array (Agilent Technologies, Palo Alto, CA). The annotation files on the platform were downloaded.

Data preprocessing and identification of DE-miRs: Based on the annotation information, the probe levels were converted into miRNA expression values. The probe that did not correspond to a specific miRNA was removed, and when more than one probe corresponded to a single miRNA, the average value at the probe level was calculated as the final expression value of this miRNA. Then the data were subjected to normalization using the median method in the [preprocess-Core](#) package [18]. Afterwards, the DE-miRs between the RB and healthy retina samples were selected using the [limma \(Linear Models for Microarray Analysis\)](#) package of R [19]. The cut-off values for significant DE-miRs were $p < 0.05$ and $|\log_2(\text{fold change})| > 0.58$.

Construction of integrated miRNA–target network: Considering that a miRNA works through the regulation of the target in a spectrum of biologic processes, we further explored the potential target genes of these identified DE-miRs, by integrating the information in two experimentally validated databases, the [miRecords](#) [20] and [MirWalk](#) [21], in which miRNA–target interactions were experimentally validated. Only the miRNA–target interaction that existed in at least one of the two databases was screened out to establish the integrated miRNA–target network.

Pathway enrichment analysis of the predicted target genes: To further identify the altered biologic pathways of the target genes, the Kyoto Encyclopedia of Genes and Genomes (KEGG) pathway enrichment analysis was conducted with the Database for Annotation, Visualization and Integration Discovery (DAVID) software [22], based on the hypergeometric distribution. $p < 0.05$ was set as the threshold for the selection of significant pathways.

Identification of transcription factors, tumor-associated genes, and tumor suppressor genes: The target genes were

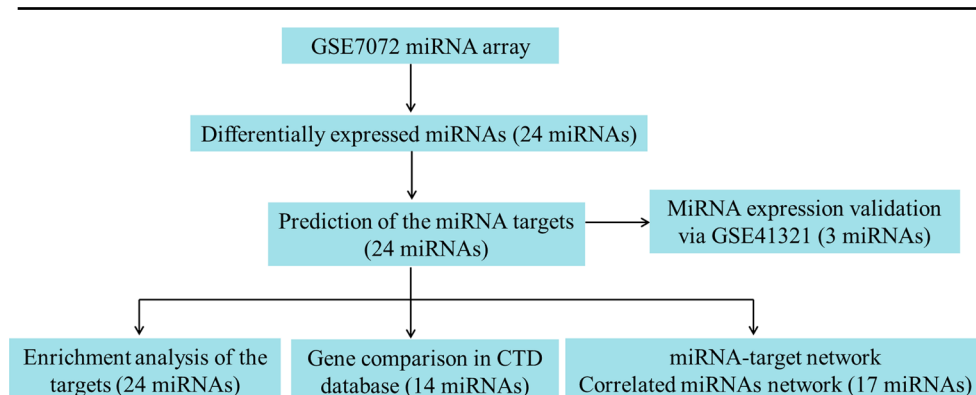


Figure 1. Flowchart of the analyses.

mapped into the TRASFAC database [23] to further screen the potential transcription factors (TFs). Meanwhile, by comparing these targets with the information from the tumor suppressor gene (TSG) [24] and tumor-associated gene (TAG) databases, all known oncogenes and TSGs among the target genes were extracted.

Prediction of RB-related genes among the target genes: The target genes were mapped into the publicly available Comparative Toxicogenomics Database (CTD) database, which provides curated chemical- and gene-disease interactions from published articles [25], to search the RB-related genes among these target genes. Then combined with the corresponding miRNAs, clustering analysis was performed between the RB and healthy retina samples with the *pvclust* package of R [26].

Correlation network construction of the identified DE-miRs: Among the DE-miRs, two miRNAs that share a common target gene were filtered out to build the correlation network.

Validation of miRNA expression with another data set: Another RB-related miRNA expression profile, GSE41321 [27], which also contained three RB samples and three healthy samples, was downloaded in the GEO database and used to check whether the DE-miRs identified in this profile were consistent with those in the GSE7072 data set. Samples in the GSE41321 profile were collected from pooled serum from children with advanced RB and healthy age-matched children. Likewise, after expression value conversion from probe level to gene level, normalization was performed for data using the median method in the *preprocessCore* package [18]. Then the miRNA expression value was attained. The *CONOR* package [28] was used to perform cross-platform normalization for the GSE7072 and GSE41321 data sets. DE-miRs between the RB and control samples were identified in the two data sets, respectively, using the *limma* package with the same threshold. Thereafter, we compared the miRNA expression in the two data sets, especially the 24 DE-miRs identified in GSE7072.

RESULTS

The DE-miRs between the RB and healthy retina samples: As a result, a set of 24 DE-miRs were selected, including nine upregulated (e.g., *hsa-miR-25*, *hsa-miR-373*, and *hsa-miR-20a*) and 15 downregulated miRNAs (e.g., *let-7b*, *let-7a*, *let-7c*, *hsa-miR-125b*, and *hsa-miR-181a*) between the RB and healthy retina samples. The clustering analysis of the heat map is presented in Figure 2, revealing the expression pattern of the DE-miRs.

The integrated miRNA–target regulatory network: Based on the criterion, the integrated miRNA–target regulatory network was built, containing five upregulated miRNAs, including *hsa-miR-373* (the most prominent one with 53 target genes), *hsa-miR-20a* (with nine target genes), *hsa-miR-18a*, *hsa-miR-25*, and *hsa-miR-175p*, and 12 downregulated miRNAs, such as *hsa-miR-125b* (the most remarkable one with 54 target genes), *hsa-miR-7 (a, b, c)*, and *hsa-miR-145* (Figure 3). Notably, *hsa-miR-20a*, *hsa-miR-18a*, and *hsa-miR-25* shared the common target gene *BCL2L11*; *hsa-miR-125b*, *hsa-miR-7a*, and *hsa-miR-7b* cotargeted the gene *LIN28A*.

Dysregulated pathways of the target genes: After the target genes were mapped into the KEGG databases, the altered pathways were identified. As shown in Table 1, the target genes of the upregulated miRNAs were significantly enriched in numerous cancer-related pathways such as pathways in cancer (hsa05200), bladder cancer (hsa05219), non-small cell lung cancer (hsa05223), and pancreatic cancer (hsa05212). The over-represented pathways for the targets of the downregulated miRNAs were also significantly correlated with various cancers, as well as the ErbB signaling pathway (hsa04012) and the cell cycle pathway (hsa04110).

Identified TFs, TAGs, and TSGs among target genes: As expected, the potential TFs, oncogenes, and TSGs were selected by comparing the targets with the information in relevant databases. Detailed gene information is presented in Table 2, in which target genes such as *CBFB* (Gene ID: 865; OMIM: 121360), *CEBPG* (Gene ID: 1054; OMIM: 138972), and *HMG2* (Gene ID: 8091; OMIM: 600698) were considered TFs; *CCNA2* (Gene ID: 890; OMIM: 123835), *CCND1* (Gene ID: 595; OMIM: 168461), and *ERBB2* (Gene ID: 2064; OMIM: 164870) were oncogenes; and *CDKN1B* (Gene ID: 1027; OMIM: 600778), *CDKN2A* (Gene ID: 1029; OMIM: 600160), and *E2F1* (Gene ID: 1869; OMIM: 189971) were TSGs.

RB-related miRNAs with their targets: A total of 183 target genes of the DE-miRs were identified. By mapping them into the CTD database, 87 were considered to correlate with RB. Additionally, these genes were targeted by 14 DE-miRs, including *hsa-miR-373*, *hsa-miR-125b*, *hsa-miR-20a*, *hsa-miR-145*, *hsa-let-7 (a, b, c)*, *hsa-miR-25*, *hsa-miR-18a*, *hsa-miR-182*, *hsa-miR-99a*, *hsa-miR-183*, *hsa-miR-451*, and *hsa-miR-181a*, which completely distinguished the RB samples from the healthy samples (Table 3 and Figure 4). Therefore, these miRNAs might be used as the biomarkers of RB.

The correlation network of the DE-miRs: The correlation network showing the common target genes of the DE-miRs is shown in Figure 5. As presented in this network, the

predominant correlated miRNA interactions were *hsa-let-7b* and *hsa-miR-125b* (the common target genes were *CDC25A*, *LIN28A*, and *CDK6*); and *hsa-miR-18a*, *hsa-miR-20a*, and *hsa-miR-25* (the common target gene was *BCL2L1*).

Validation of miRNA expression: As shown in Table 4, in comparison with the GSE7072 profile, ten miRNAs, including six identified DE-miRs (out of the 24 DE-miRs), were also differentially expressed in the RB samples in the GSE41321 profile. Notably, the expression of three DE-miRs, including upregulated *hsa-miR-18a* and downregulated *hsa-let-7b* and *hsa-let-7c*, was in accordance with our results.

DISCUSSION

RB is a primary pediatric cancer of the retina. In this study, we performed a series of analyses using powerful bioinformatics methods and finally identified a total of 24 DE-miRs between the RB and healthy retina samples. Interestingly, nine DE-miRs, including *let-7c*, *hsa-miR-182*, *hsa-miR-99b*, *hsa-miR-125b*, *hsa-miR-191*, *hsa-miR-181a*, *hsa-miR-17-5p*, *hsa-miR-373*, and *let-7b*, were consistent with work

performed by Huang et al. [17], who identified 25 DE-miRs in RB samples. The potential reasons for the other different miRNAs might be due to different selection criteria. As Huang et al. aimed to discover the interacting miRNA–target relationships using paired miRNA and mRNA expression profiles, they might have applied a different criterion to choose the interacting miRNA target. In contrast, this study used their miRNA expression profile and predicted the corresponding targets based on the miRecords and MirWalk databases. However, the nine common DE-miRs suggest that our findings are also reliable.

Interestingly, the expression of three DE-miRs was consistent with that in another profile, GSE41321, including *hsa-miR-18a*, *hsa-let-7b*, and *hsa-let-7c*. Although the GSE41321 samples are collected from serum, Beta et al. confirmed that a set of 33 deregulated miRNAs, such as the upregulated *hsa-miR-18a* and the downregulated *hsa-let-7c*, are also found in RB tumor samples in comparison with the tumor RB miRNA profiles [27]. This finding indicates several miRNAs in serum might have the same expression patterns as in tumors and could be used as potential biomarkers for

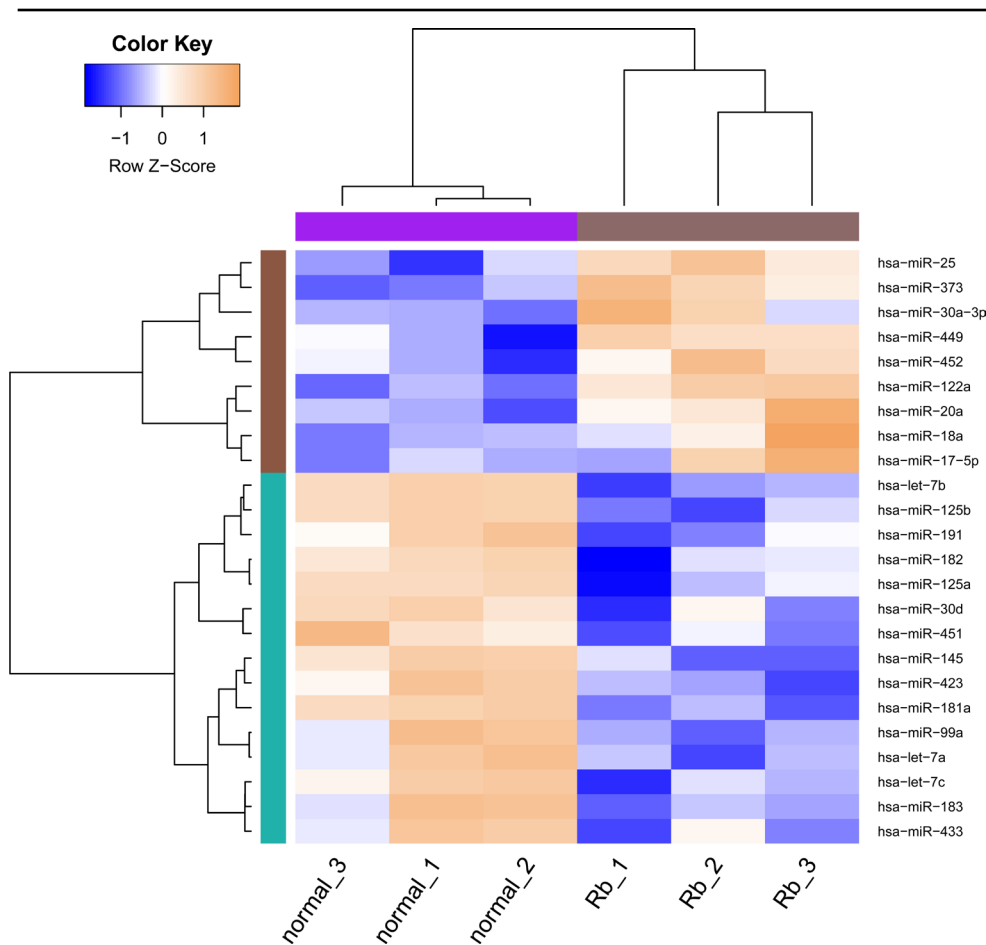


Figure 2. Heat map of the clustering analysis of differentially expressed miRNAs between two samples. The x-axis represents the samples (healthy 1–3 denote healthy retina samples, and Rb 1–3 denote retinoblastoma samples), and the y-axis represents miRNAs.

TABLE 2. PREDICTED TFs, ONCOGENES AND TSGs AMONG THE TARGET GENES OF THE DIFFERENTIALLY EXPRESSED miRNAs.

TF	Oncogene	TSG
CBFB,CEBPG,HMGA2,HOXA11,ID1,ID2,ID3,MEF2D,MITF,PLAGL1,PRDM1,ARG,RUNX1,SOX9,TFAP4,ZHX1	CCNA2,CCND1,ERBB2,ERBB3,ESR1,FGFR3,HMGA2,HRAS,KRAS,MYC,NRAS	CDKN1B,CDKN2A,E2F1,FOXO1,ITGB3,LATS2,MAP2K4,NF2,PLAGL1,PPP1CA,PRDM1,RECK,SMO,TP53,TP53INP1,TUSC2,UHRF2

TF: transcription factor; TSG: tumor suppressor gene.

shared the common target gene *BCL2L11*; *hsa-let-7b* and *hsa-miR-125b* targeted three genes, *CDC25A*, *CDK6*, and *LIN28A*.

MiR-373 is implicated in numerous cancer events. Previously, *miR-373-3* was considered the signature of human embryonic stem cells [29]. In prostate cancer, in vitro experiments showed that *miR-373* stimulates cell migration and invasion [30]. Additionally, the role of *miR-373* as an activator in tumor invasion and metastasis has been verified in vivo and in vitro by inhibiting the expression of *CD44* [31]. Furthermore, *miR-373* is proproliferative in human epithelial ovarian cancer cells [32]. Several studies corroborated that *miR-373* is highly expressed in RB tumors, in comparison with healthy retinas [12,33], which is consistent with our result. Notably, our enrichment analysis showed that the targets of *hsa-miR-373* were tightly correlated with a cohort of cancer-related pathways, providing potent evidence that *hsa-miR-373* might function in RB tumors as in other cancers. Given that RB has a tendency toward local invasion and metastasis [34], it might

be speculated that *miR-373* might also play remarkable roles in the regulation of RB invasion and metastasis.

Defects in the gene *RBI*, which serves as a negative regulator of cell cycle and a tumor suppressor, are known to be the main cause for the genesis of RB in children. A cluster of miRNAs acts as regulators in cell proliferation, apoptosis, and senescence via interfering with the p53 pathway or *RBI/E2F* function [35,36]. *MiR-125b* has been confirmed to function as a tumor suppressor by inducing cellular senescence in cutaneous malignant melanoma [37]. Notably, *miR-125b* is closely related to the p53 pathway in colorectal cancer [38]. These collectively provide a clue that *miR-125b* might also be involved in the regulation of proliferation during RB development via the p53-mediated pathway. In human U251 glioma stem cells, the overexpression of *miR-125b* is highly correlated with the decreased expression of *CDK6* and *CDC25A*, two cell cycle-mediated genes [39]. Moreover, *CDK6* and *CDC25A* are mediated by *miR-125b* in other types of cancer, such as breast cancer [40] and bladder cancer [41]. The oncogene *LIN28B*

TABLE 3. RETINOBLASTOMA-RELATED miRNAs AND THEIR TARGET GENES.

miRNAs	Target genes
hsa-miR-373	GPSM2, KIF23, GLTP, LATS2, TFAP4, GBP3, PRC1, LMNB1, RNF149, INSIG2, TEX30, CYB5R4, RPIA, PBK, STK4, KDM1B, CENPF, TBC1D2, ARHGEF3, CD83
hsa-miR-125b	ID2, CASP6, ADAMTS1, NTRK3, ID3, JARID2, CBX7, UGT2B17, ELAVL1, BAK1, EIF4EBP1, TENM2, E2F3, MAN1A1, KRT19, TP53INP1, TP53, CDC25A, CDKN2A, CDK6, SMO, BMPR1B, CYP1A1, CASP7, BBC3, CBLN2, UBE2I, IL1RN, B3GALT4, CDC25C, ERBB3, ERBB2, PIGR
hsa-miR-20a	BCL2L11, CCND1, BMPR2, RUNX1, E2F1, MAP3K12
hsa-let-7b	CDC25A, CDK6, CCND1, HMGA2, KRT19
hsa-miR-145	FSCN1, SOX9, IGF1R, RTKN, CCNA2, MYC, PPP3CA
hsa-let-7a	NF2, SMOX, KRAS, ITGB3, CASP3, HMGA2, HRAS, NRAS
hsa-miR-182	MITF, IGF1R, RARG
hsa-miR-99a	MTOR, IGF1R, FGFR3
hsa-miR-25	MAP2K4, BCL2L11
hsa-miR-18a	CTGF, BCL2L11, ESR1
hsa-miR-181a	CDKN1B, ESR1
hsa-miR-183	FOXO1
hsa-let-7c	MYC, HMGA2
hsa-miR-451	ABCBI

Cluster dendrogram with AU/BP values (%)

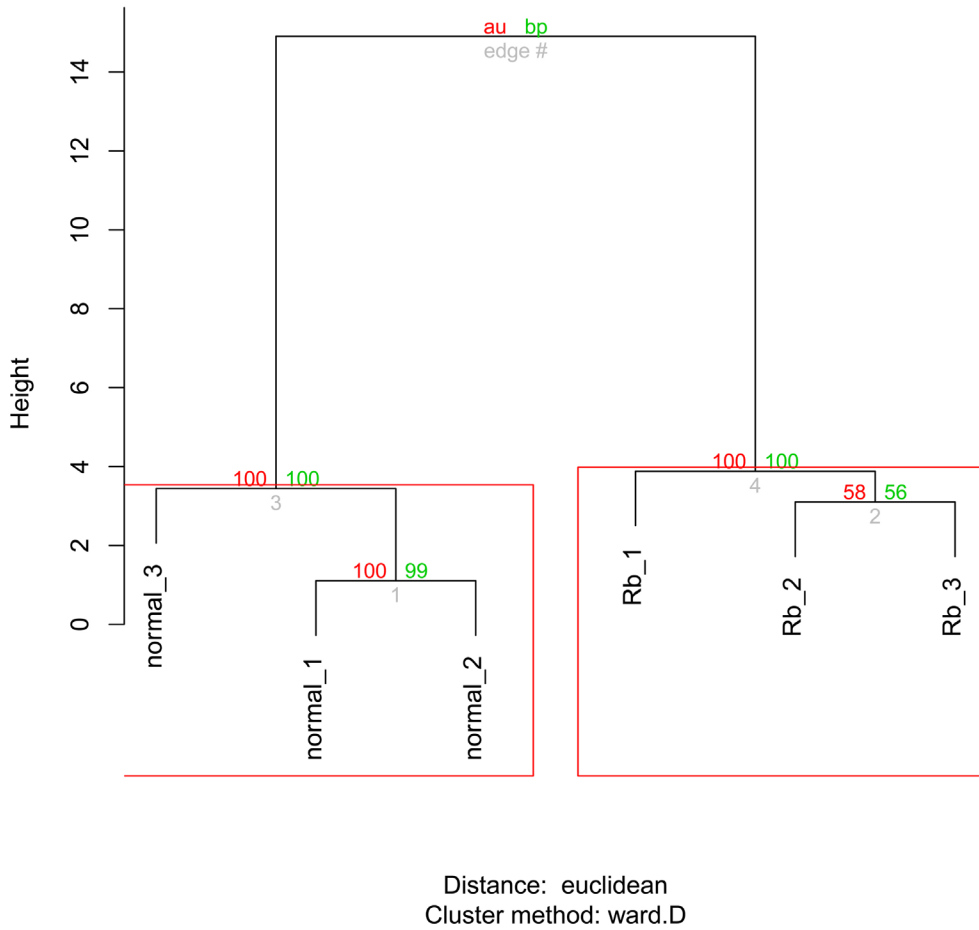


Figure 4. Clustering analysis of the 14 differentially expressed miRNAs in two types of samples. Healthy 1–3 denote the healthy retina samples, and Rb 1–3 denote the retinoblastoma samples. The values on the edges of the clusters are p values (%). The red values are approximately unbiased (au) p values, and the green values are bootstrap probability (bp) values. Clusters with au larger than 95% are highlighted by rectangles, which are strongly supported by data.

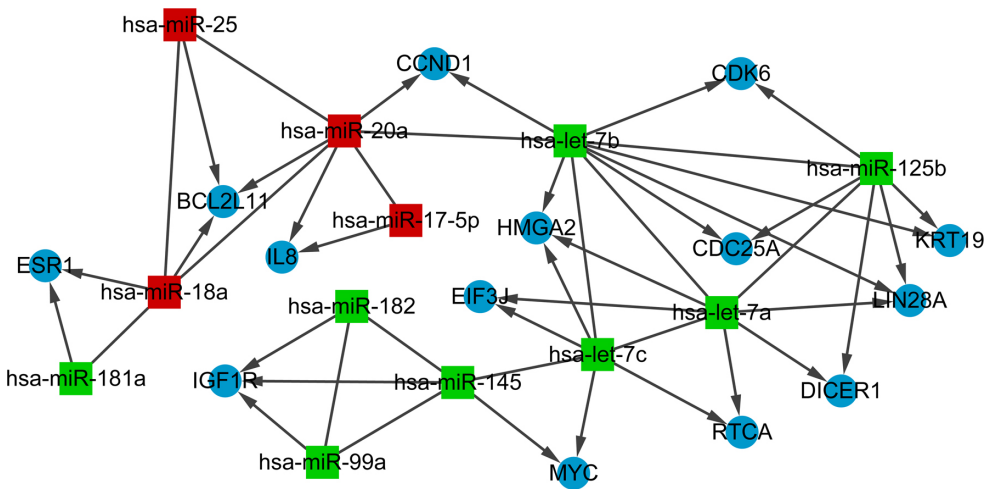


Figure 5. Correlation network of the differentially expressed miRNAs. The blue circle represents genes, and the red rectangle represents up-regulated miRNAs, while the green rectangle represents down-regulated miRNAs. The arrow denotes the direct interaction between miRNA and its target gene.

has been demonstrated to be the downstream of *miR-125b*, and by binding to the 3' untranslated region (UTR) region of *LIN28B*, *miR-125b* successfully inhibited the cell growth in hepatocellular carcinoma [42]. The regulatory relationships between *hsa-let-7b* and the target *CDC25A* have been well established in RB cells [17]. Additionally, *let-7* is suggested to indirectly regulate the cell cycle by suppressing *IMPI*, an essential gene for *CDC25A* and *CDK6* expression [43]. Furthermore, *let-7* could also downregulate the mRNA of *LIN28B* during neural stem cell commitment [44]. Interestingly, our results showed that *CDK6*, *CDC25A*, and *LIN28A*, the paralog of *LIN28B*, were all targeted by *miR-125b* and *hsa-let-7b*, indicating these two miRNAs might play crucial roles in the development of RB, via the coregulation of the three cell cycle-related target genes.

Hsa-miR-181b and *hsa-miR-181a* are downregulated in human gliomas and have been implicated as tumor suppressors by inhibiting glioma proliferation [45]. In RB cells, elevated *miR-181b* has been verified to play a positive role in RB cell proliferation under hypoxic conditions [46]. Considering that RB is a cancer of the nervous system and *miR-181b* is dysregulated in the central nervous system disease schizophrenia, *miR-181b* has been suggested to be involved in the genesis of RB [46]. In addition, *miR-181a*, along with *miR-183* and *miR-124*, presents the most frequent alterations among the miRNAs differentially expressed in RB [47]. The *CDKN1B* gene, an important regulator of the cell cycle, has been demonstrated as the target of *miR-221* and *miR-222* in the development of thyroid cancer [48]. Our results indicated that *hsa-miR-181a* was a crucial miRNA of RB that targeted

multiple genes, including *CDKN1B*, which was predicted to be a TSG enriching in the cell cycle pathway. Therefore, it might be inferred that *hsa-miR-181a* might act as an important regulator in RB progression via the *CDKN1B*-mediated cell cycle pathway.

The *BCL2L1* encoded protein belongs to the BCL-2 protein family, which act as important apoptotic activators in extensive cellular activities [49]. Transforming growth factor- β (TGF- β) is a cytokine that has a significant role in the apoptosis of gastrointestinal cells. *miR-25* overexpression decreases TGF β -induced apoptosis by interfering with the synthesis of *BCL2L1* in gastric cancer [50]. Additionally, *miR-20a* has also been reported to target *BCL2L1*, while *miR-18a* could target *Smad2* and *Smad4* in the TGF- β signaling pathway, in which the activation of TGF- β is partly regulated by *BCL2L1* [51]. In the present study, *hsa-miR-25*, *hsa-miR-18a*, and *hsa-miR-20a* simultaneously targeted *BCL2L1* in the correlation network of the DE-miRs, suggesting that the three miRNAs might have vital roles in the progression of RB by coregulating *BCL2L1*. However, the potential interactions between these miRNAs must be further elucidated.

The present study has several limitations. First, the sample size was small because only three RB samples and three healthy samples were contained in the data sets. Moreover, although we used another data set to validate the miRNA expression, the expression of only three miRNAs was confirmed. Experimental validation of miRNA expression and miRNA-target regulation was lacking, which will be considered in follow-up studies.

TABLE 4. miRNA (10 DE-miRs) EXPRESSION COMPARISON BETWEEN EXPRESSION PROFILES OF GSE41321 AND GSE7072.

miRNAs	GSE41321		GSE7072	
	Log FC	P value	Log FC	P value
hsa-miR-30d	0.699283069	8.34E-06	-1.4135091	1.28E-02
hsa-miR-18a	0.820197258	3.05E-05	1.486038867	3.38E-02
hsa-miR-181a	0.872595328	1.01E-06	-1.9342523	5.73E-04
hsa-miR-183	0.561178808	1.26E-04	-1.2667168	1.94E-02
hsa-miR-182	0.95936798	5.54E-07	-1.24761365	2.40E-02
hsa-miR-125b	0.457144179	4.40E-04	-2.520854685	3.56 E-04
hsa-miR-191	-0.483798552	1.04E-03	-1.80388745	7.45E-03
hsa-miR-373	-0.109119276	0.20	1.196955933	9.69E-03
hsa-let-7c	-0.838050781	6.21E-05	-2.213052267	3.67E-03
hsa-let-7b	-0.704607286	4.49E-05	-3.044672233	9.35E-05

DE-miRs: differentially expressed miRNAs (between retinoblastoma and control samples); FC: fold change; miRNAs with positive value of Log FC represent upregulated miRNAs in retinoblastoma samples; while with negative value indicate downregulated miRNAs in retinoblastoma samples.

In conclusion, a set of critical miRNA signatures was identified in RB progression. Among them, *hsa-miR-373* might play significant roles in the regulation of RB invasion and metastasis, *hsa-miR-125b* and *hsa-let-7b* might exert their roles as tumor suppressors via the coregulation of *CDK6*, *CDC25A*, and *LIN28A*, which all mediated the cell cycle pathway, and *hsa-miR-181a* might involve in the *CDKN1B*-regulated cell cycle pathway. Additionally, *hsa-miR-25*, *hsa-miR-18a*, and *hsa-miR-20a* might affect the progression of RB by the coregulation of *BCL2L1*. However, additional experimental studies are needed to confirm these results.

ACKNOWLEDGMENTS

This work was supported by Hubei Provincial Natural Science Foundation of China (No. 2014CFB366).

REFERENCES

- Wong JR, Tucker MA, Kleinerman RA, Devesa SS. Retinoblastoma incidence patterns in the US Surveillance, Epidemiology, and End Results program. *JAMA Ophthalmol* 2014; 132:478-83. [PMID: 24577366].
- Waddell KM, Kagame K, Ndamira A, Twinamasiko A, Picton SV, Simmons IG, Johnston WT, Newton R. Clinical features and survival among children with retinoblastoma in Uganda. *Br J Ophthalmol* 2015; 99:387-90. [PMID: 25217695].
- Park SJ, Woo SJ, Park KH. Incidence of Retinoblastoma and Survival Rate of Retinoblastoma Patients in Korea Using the Korean National Cancer Registry Database (1993–2010) Incidence and Survival of Retinoblastoma in Korea. *Invest Ophthalmol Vis Sci* 2014; 55:2816-21. [PMID: 24692122].
- Li S-Y, Chen SC-C, Tsai C-F, Sheu S-M, Yeh J-J, Tsai C-B. Incidence and survival of retinoblastoma in Taiwan: a nationwide population-based study 1998–2011. *Br J Ophthalmol* 2015; xxx:307211-[PMID: 26370121].
- Pritchard EM, Dyer M, Guy R. Progress in Small Molecule Therapeutics for the Treatment of Retinoblastoma. *Mini Rev Med Chem* 2015; [PMID: 26202204].
- Chantada GL, Qaddoumi I, Canturk S, Khetan V, Ma Z, Kimani K, Yeniad B, Sultan I, Sitorus RS, Tacyildiz N. Strategies to manage retinoblastoma in developing countries. *Pediatr Blood Cancer* 2011; 56:341-8. [PMID: 21225909].
- Zhang J, Benavente CA, McEvoy J, Flores-Otero J, Ding L, Chen X, Ulyanov A, Wu G, Wilson M, Wang J. A novel retinoblastoma therapy from genomic and epigenetic analyses. *Nature* 2012; 481:329-34. [PMID: 22237022].
- Li B-Q, Zhang J, Huang T, Zhang L, Cai Y-D. Identification of retinoblastoma related genes with shortest path in a protein-protein interaction network. *Biochimie* 2012; 94:1910-7. [PMID: 22627383].
- Gayral M, Jo S, Hanoun N, Vignolle-Vidoni A, Lulka H, Delpu Y, Meulle A, Dufresne M, Humeau M, du Rieu MC. MicroRNAs as emerging biomarkers and therapeutic targets for pancreatic cancer. *World J Gastroenterol* 2014; 20:11199- [PMID: 25170204].
- Vannini I, Fanini F, Fabbri M. MicroRNAs as lung cancer biomarkers and key players in lung carcinogenesis. *Clin Biochem* 2013; 46:918-25. [PMID: 23396164].
- Liu SS, Wang YS, Sun YF, Miao LX, Wang J, Li YS, Liu HY, Liu QL. Plasma microRNA-320, microRNA-let-7e and microRNA-21 as novel potential biomarkers for the detection of retinoblastoma. *Biomed Rep* 2014; 2:424-8. [PMID: 24748987].
- Zhao J-J, Yang J, Lin J, Yao N, Zhu Y, Zheng J, Xu J, Cheng JQ, Lin J-Y, Ma X. Identification of miRNAs associated with tumorigenesis of retinoblastoma by miRNA microarray analysis. *Childs Nerv Syst* 2009; 25:13-20. [PMID: 18818933].
- Wu X, Zeng Y, Wu S, Zhong J, Wang Y, Xu J. MiR-204, down-regulated in retinoblastoma, regulates proliferation and invasion of human retinoblastoma cells by targeting CyclinD2 and MMP-9. *FEBS Lett* 2015; 589:645-50. [PMID: 25647033].
- Martin J, Bryar P, Mets M, Weinstein J, Jones A, Martin A, Vanin EF, Scholtens D, Costa FF, Soares MB. Differentially expressed miRNAs in retinoblastoma. *Gene* 2013; 512:294-9. [PMID: 23103829].
- Conkrite K, Sundby M, Mukai S, Thomson JM, Mu D, Hammond SM, MacPherson D. miR-17-92 cooperates with RB pathway mutations to promote retinoblastoma. *Genes Dev* 2011; 25:1734-45. [PMID: 21816922].
- Guha N, Deepak S, Lateef S, Padmanabhan A, Gundimeda S, Ghosh A, Mallipatna A, Babu VS. A Multi-omics Approach to Identify Biomarkers of Clinically Advanced Retinoblastoma for Diagnostics and Therapeutic Applications. *FASEB J* 2015; 29:417-.
- Huang JC, Babak T, Corson TW, Chua G, Khan S, Gallie BL, Hughes TR, Blencowe BJ, Frey BJ, Morris QD. Using expression profiling data to identify human microRNA targets. *Nat Methods* 2007; 4:1045-9. [PMID: 18026111].
- Bolstad BM, Irizarry RA, Åstrand M, Speed TP. A comparison of normalization methods for high density oligonucleotide array data based on variance and bias. *Bioinformatics* 2003; 19:185-93. [PMID: 12538238].
- Smyth GK. Limma: linear models for microarray data. *Bioinformatics and computational biology solutions using R and Bioconductor*: Springer; 2005. p. 397–420.
- Xiao F, Zuo Z, Cai G, Kang S, Gao X, Li T. miRecords: an integrated resource for microRNA–target interactions. *Nucleic Acids Res* 2009; 37:D105-10. [PMID: 18996891].
- Dweep H, Sticht C, Pandey P, Gretz N. miRWalk–database: prediction of possible miRNA binding sites by “walking” the genes of three genomes. *J Biomed Inform* 2011; 44:839-47. [PMID: 21605702].
- Dennis G Jr, Sherman BT, Hosack DA, Yang J, Gao W, Lane HC, Lempicki RA. DAVID: database for annotation, visualization, and integrated discovery. *Genome Biol* 2003; 4:3-[PMID: 12734009].

23. Matys V, Kel-Margoulis OV, Fricke E, Liebich I, Land S, Barre-Dirrie A, Reuter I, Chekmenev D, Krull M, Hornischer K. TRANSFAC® and its module TRANSCompel®: transcriptional gene regulation in eukaryotes. *Nucleic Acids Res* 2006; 34:D108-10. [PMID: 16381825].
24. Zhao M, Sun J, Zhao Z. TSGene: a web resource for tumor suppressor genes. *Nucleic Acids Res* 2013; 41:D970-76. [PMID: 23066107].
25. Wieggers TC, Davis AP, Cohen KB, Hirschman L, Mattingly CJ. Text mining and manual curation of chemical-gene-disease networks for the comparative toxicogenomics database (CTD). *BMC Bioinformatics* 2009; 10:326-[PMID: 19814812].
26. Suzuki R, Shimodaira H. Pvcust: an R package for assessing the uncertainty in hierarchical clustering. *Bioinformatics* 2006; 22:1540-2. [PMID: 16595560].
27. Beta M, Venkatesan N, Vasudevan M, Vetrivel U, Khetan V, Krishnakumar S. Identification and insilico analysis of retinoblastoma serum microRNA profile and gene targets towards prediction of novel serum biomarkers. *Bioinform Biol Insights* 2013; 7:21-[PMID: 23400111].
28. Rudy J, Valafar F. Empirical comparison of cross-platform normalization methods for gene expression data. *BMC Bioinformatics* 2011; 12:467-[PMID: 22151536].
29. Ren J, Jin P, Wang E, Marincola FM, Stroncek DF. MicroRNA and gene expression patterns in the differentiation of human embryonic stem cells. *J Transl Med* 2009; 7:20-[PMID: 19309508].
30. Yang K, Handorean AM, Iczkowski KA. MicroRNAs 373 and 520c are downregulated in prostate cancer, suppress CD44 translation and enhance invasion of prostate cancer cells in vitro. *Int J Clin Exp Pathol* 2009; 2:361-[PMID: 19158933].
31. Huang Q, Gumireddy K, Schrier M, Le Sage C, Nagel R, Nair S, Egan DA, Li A, Huang G, Klein-Szanto AJ. The microRNAs miR-373 and miR-520c promote tumour invasion and metastasis. *Nat Cell Biol* 2008; 10:202-10. [PMID: 18193036].
32. Nakano H, Yamada Y, Miyazawa T, Yoshida T. Gain-of-function microRNA screens identify miR-193a regulating proliferation and apoptosis in epithelial ovarian cancer cells. *Int J Oncol* 2013; 42:1875-82. [PMID: 23588298].
33. Reis AH, Vargas FR, Lemos B. More epigenetic hits than meets the eye: microRNAs and genes associated with the tumorigenesis of retinoblastoma. *Front Genet* 2012; 3:284-[PMID: 23233862].
34. Chen X, Wang J, Cao Z, Hosaka K, Jensen L, Yang H, Sun Y, Zhuang R, Liu Y, Cao Y. Invasiveness and metastasis of retinoblastoma in an orthotopic zebrafish tumor model. *Sci Rep* 2015; 5:10351-[PMID: 26169357].
35. Farh KK-H, Grimson A, Jan C, Lewis BP, Johnston WK, Lim LP, Burge CB, Bartel DP. The widespread impact of mammalian MicroRNAs on mRNA repression and evolution. *Science* 2005; 310:1817-21. [PMID: 16308420].
36. Kato M, Slack FJ. microRNAs: small molecules with big roles—C. elegans to human cancer. *Biol Cell* 2008; 100:71-81. [PMID: 18199046].
37. Nyholm AM, Lerche CM, Manfé V, Biskup E, Johansen P, Morling N, Thomsen BM, Glud M, Gniadecki R. miR-125b induces cellular senescence in malignant melanoma. *BMC Dermatol* 2014; 14:8-[PMID: 24762088].
38. Nishida N, Yokobori T, Mimori K, Sudo T, Tanaka F, Shibata K, Ishii H, Doki Y, Kuwano H, Mori M. MicroRNA miR-125b is a prognostic marker in human colorectal cancer. *Int J Oncol* 2011; 38:1437-43. [PMID: 21399871].
39. Shi L, Zhang J, Pan T, Zhou J, Gong W, Liu N, Fu Z, You Y. MiR-125b is critical for the suppression of human U251 glioma stem cell proliferation. *Brain Res* 2010; 1312:120-6. [PMID: 19948152].
40. Zhang Y, Yan L-X, Wu Q-N, Du Z-M, Chen J, Liao D-Z, Huang M-Y, Hou J-H, Wu Q-L, Zeng M-S. miR-125b is methylated and functions as a tumor suppressor by regulating the ETS1 proto-oncogene in human invasive breast cancer. *Cancer Res* 2011; 71:3552-62. [PMID: 21444677].
41. Chen H, Lin Y-W, Mao Y-Q, Wu J, Liu Y-F, Zheng X-Y, Xie L-P. MicroRNA-449a acts as a tumor suppressor in human bladder cancer through the regulation of pocket proteins. *Cancer Lett* 2012; 320:40-7. [PMID: 22266187].
42. Liang L, Wong CM, Ying Q, Fan DNY, Huang S, Ding J, Yao J, Yan M, Li J, Yao M. MicroRNA-125b suppressed human liver cancer cell proliferation and metastasis by directly targeting oncogene LIN28B2. *Hepatology* 2010; 52:1731-40. [PMID: 20827722].
43. Barh D. Let-7 replacement therapy: applicability in cancer. *Cancer Ther* 2008; 6:969-84. .
44. Rybak A, Fuchs H, Smirnova L, Brandt C, Pohl EE, Nitsch R, Wulczyn FG. A feedback loop comprising lin-28 and let-7 controls pre-let-7 maturation during neural stem-cell commitment. *Nat Cell Biol* 2008; 10:987-93. [PMID: 18604195].
45. Shi L, Cheng Z, Zhang J, Li R, Zhao P, Fu Z, You Y. hsa-mir-181a and hsa-mir-181b function as tumor suppressors in human glioma cells. *Brain Res* 2008; 1236:185-93. [PMID: 18710654].
46. Xu X, Jia R, Zhou Y, Song X, Wang J, Qian G, Ge S, Fan X. Microarray-based analysis: identification of hypoxia-regulated microRNAs in retinoblastoma cells. *Int J Oncol* 2011; 38:1385-93. [PMID: 21373755].
47. Wang J, Wang X, Li Z, Liu H, Teng Y. MicroRNA-183 suppresses retinoblastoma cell growth, invasion and migration by targeting LRP6. *FEBS J* 2014; 281:1355-65. [PMID: 24289859].
48. Marini F, Luzi E, Brandi ML. MicroRNA Role in Thyroid Cancer Development. *J Thyroid Res* 2011; 2011:407123-[PMID: 21687652].
49. Michelle L, Cloutier A, Toutant J, Shkreta L, Thibault P, Durand M, Garneau D, Gendron D, Lapointe E, Couture S. Proteins associated with the exon junction complex also

- control the alternative splicing of apoptotic regulators. *Mol Cell Biol* 2012; 32:954-67. [PMID: 22203037].
50. Petrocca F, Visone R, Onelli MR, Shah MH, Nicoloso MS, De Martino I, Iliopoulos D, Pilozzi E, Liu C-G, Negrini M. E2F1-regulated microRNAs impair TGF β -dependent cell-cycle arrest and apoptosis in gastric cancer. *Cancer Cell* 2008; 13:272-86. [PMID: 18328430].
51. Mogilyansky E, Rigoutsos I. The miR-17/92 cluster: a comprehensive update on its genomics, genetics, functions and increasingly important and numerous roles in health and disease. *Cell Death Differ* 2013; 20:1603-14. [PMID: 24212931].

Articles are provided courtesy of Emory University and the Zhongshan Ophthalmic Center, Sun Yat-sen University, P.R. China. The print version of this article was created on 14 December 2015. This reflects all typographical corrections and errata to the article through that date. Details of any changes may be found in the online version of the article.